AN AHRS BASED ON A KALMAN FILTER FOR THE INTEGRATION OF INERTIAL, MAGNETOMETRIC AND GPS DATA

Eugenio Denti, Roberto Galatolo, Francesco Schettini
University of Pisa, Italy– Department of Aerospace Engineering
Keywords: *Kalman filter, MEMS, sensors integration*

Abstract

The paper describes an Attitude & Heading Reference System able to achieve a high accuracy level by using a Kalman filter, which integrates the measurements coming from low cost inertial sensors, magnetometric sensors and a GPS receiver. The errors correction on attitude and heading angles, calculated through the integration of the gyroscopes measurements, is performed on the basis of their alternative estimation. Such values are provided by a model which uses magnetometric measurements and accurate estimation of the gravity vector, calculated by purging the aircraft acceleration effect from the accelerometers measurements. An estimation of aircraft acceleration is obtained tanks to velocity information coming from GPS measurements.
The system performance has been evaluated through simulation tests in which the input signals were time histories of acceleration, velocity and position generated by a flight simulator.

1 Introduction

An Attitude & Heading Reference System (AHRS) is a self-contained system which provides the pitch, roll and yaw angles, thus combining the gyro-compass and artificial horizon functions. This system is used in many fields: aerial, terrestrial and nautical, and its outputs can be provided to the pilot, control systems or other avionics devices. In particular, the developed AHRS has to guarantee high accuracy outputs in all operative conditions of high performance aircraft or UAV. In the past, the sensors embedded in the AHRSs were very expensive and thus their usage was limited to military and aerospace applications. However, the recent advance of Micro Electric Mechanical System technologies (MEMS), makes the AHRSs smaller in size and cheaper.
Low cost sensors exhibit low accuracy and noisy outputs, so their application is possible only by using proper techniques for errors correction. Many of such techniques are based on multi-sensor architectures which allow the variables estimation by means of the synergy of information coming from different measurement sources, characterized by different kind of errors (low frequency with a high accuracy/high frequency with errors rapidly growing). The hardware solution considered in the paper is constituted by a three-axis MEMS gyroscope, a three-axis MEMS accelerometer, a three-axis magnetometer (all installed on a strapdown platform), and by a temperature sensor and a GPS receiver.

2 Measurement Errors

Sensor measurements are affected by different types of errors, depending on the principle of functioning, on the measurement signal transmission and on the devices manufacturing imperfections. The errors analysis allows the effect of each type of error on the system performance to be determined.

2.1 Sensors Errors

Tab. 1 shows typical errors of MEMS accelerometers and gyroscopes, and

magnetometers. The main error sources are ([1], [2], [3], [4]):

- *Misalignment.* It is caused by the fact that the triads of sensors are never perfectly orthogonal, due to assembling imperfections and thermal deformations. As a consequence, each sensor provides data not only depending on the input along the body axis to which it is nominally aligned, but also on the inputs along the other orthogonal directions.
- *Bias.* Theoretically, the sensor output should be zero for null inputs. In practice, the output differs from zero of a value, named *bias*, characterized by four contributes:
  - a constant value (*Constant Bias*);
  - a value which represents the variation of the bias at each power up (*Long Term Bias Stability*), also due to sensors wear;
  - a value which represents the oscillation over short time, about 100 seconds (*Short Term Bias Stability*);
  - a value depending on the working temperature of the sensor (*Bias Temperature Shift*).
- *Noise.* It results from many small sources of disturbance which cause rapid and unpredictable fluctuations of the output signal. The main sources are electrical and mechanical, the latter due to frictions and vibrations. Typically, this kind of error is modelled as white noise, characterized by a null average and a variance given by the product between spectral density (S_W) and sensor bandwidth (B_W).
- *Scale Factor*. Such an error represents the variation of the calibration curve slope and it mainly depends on the sensor working temperature.
- *G and G^2 Sensitivity*. On the basis of the sensors working principle, they can be more or less sensitive to the acceleration with linear or quadratic laws.

2.2 GPS Errors

There are several factors which determine inaccuracies in the values of position provided by a GPS receiver ([2], [3], [5], [6]). The pseudo-range, that is the distance between the receiver and a generic satellite, is affected by errors due to the inaccuracies of atomic clock aboard of the satellites and the approximate knowledge of the orbital parameters of the satellites (errors introduced by the ephemeris data).

	Gyroscopes	Accelerometers	Magnetometers
Input range	±1000 [°/s]	±70*9.81 [m/s^2]	2e5 [nT]
Bandwidth	50 [Hz]	50 [Hz]	50 [Hz]
Constant and Long Term Bias Stability (σ)	15/3600 [°/s]	9.81e-3 [m/s^2]	20 [nT]
Short Term Bias Stability (σ) (τ_{STBS})	5/3600 [°/s] (300 s)	9.81e-3 [m/s^2] (300 s)	4 [nT] (300 s)
Bias Temperature Shift ($T_{reference}$)	2e-4 [(°/s)/°C] (25 °C)	9.81e-4 [(m/s^2)/°C] (25 °C)	20e-4 [nT/°C] (25 °C)
Scale Factor (σ)	150 [ppm]	300 [ppm]	500 [ppm]
G Sensitivity	3/3600 [(°/s)/g]	0	0
G^2 Sensitivity	0.6/3600 [(°/s)/g^2]	0	0
Noise (S_W)	(0.1/60)^2 [(°/s)^2/Hz]	(0.22/60)^2 [(m/s^2)^2/Hz]	(0.7)^2 [nT^2/Hz]
Misalignment (σ)	50/sqrt(2) [μrad]	100/sqrt(2) [μrad]	12000/sqrt(2) [μrad]

Tab. 1. Error parameters of gyroscopes, accelerometers and magnetometers

In addition, there are errors caused by the multipath effect, the propagation of the signals across the ionosphere and troposphere, and by the measurement noise. The position accuracy calculated by the receiver also depends on the Dilution of Precision (DOP) effect. The DOP is a geometric effect depending on the position of the satellites and the receiver at the moment in which the computation is carried out. Such an effect is taken into account through proper coefficients multiplying the pseudo-range error.
The GPS receiver considered in this work has a data updating frequency of 4 Hz. Tab. 2 shows the position error standard deviation in the horizontal and vertical planes, and the pseudo-range standard deviation errors (σ) for the different error sources. For each contribute, two terms are indicated: one of bias type and another of random type.

Sources	σ_{Bias} [m]	σ_{Random} [m]	σ_{Totale} [m]
Ephemeris	2.1	0.0	2.1
Satellite clock	2.0	0.7	2.1
Ionosphere	4.0	0.5	4.0
Troposphere	0.5	0.5	0.7
Multi-path	1.0	1.0	1.4
Receiver	0.5	0.2	0.5
UERE	5.1	1.4	5.3
Horiz. position error - HDOP·UERE (HDOP=2.1)			11.1
Vertical position error - DDOP·UERE (DDOP=2.5)			13.3

Tab. 2. Standard deviations of the pseudoranges and receiver position

By assuming that all the phenomena are independent and with a null average, that is valid over a long time of observation, such as dozens hours or days, the overall error, named UERE (*User Equivalent Range Error*), can be evaluated by summing the root square of the various contributes.

As far as the GPS velocity error is concerned, it is not easy to find information in the literature. Results in [7] show that such an error increases if an acceleration acts on the receiver. Under constant velocity (20÷25 mph), the standard deviation error on the velocity is equal to 0.03 m/sec northward and eastward, and 0.05 m/sec along the vertical direction. On the contrary, the error grows to 2 m/sec in the presence of accelerations of 2÷3 g (e.g. missiles systems).

3 AHRS Architecture

The developed architecture (Fig. 1) is constituted by a computation unit which elaborates the signals coming from the sensors and the GPS receiver. The temperature sensor is used to compensate the temperature effects on the inertial measurements on the basis of laws provided by the inertial sensors manufacturer.

The AHRS working principle is based on the Kalman filter which determines the optimum estimation of the Euler angles of roll, pitch and yaw (θ, φ, ψ) by using two independent information sources: the first one, "*Attitude & Heading Estimations*" block, provides the high-frequency values of the unknown variables thanks to the integration of the angular velocities coming from gyroscopes; the second one, "*Attitude & Heading Measurements*" block, provides low-frequency values tanks to a specific computation model based on: the accelerometers and magnetometers measurements, the GPS data and the values of the magnetic field coming from the *World Magnetic Model* (WMM) [8]. The Kalman filter allows high frequency data to be compensated thanks to more precise low-frequency information.

3.1 Attitude & Heading Estimations

The block integrates the following differential equation:

$$\begin{bmatrix}\dot{q}_0\\ \dot{q}_1\\ \dot{q}_2\\ \dot{q}_3\end{bmatrix}=\frac{1}{2}\begin{bmatrix}0 & -p & -q & -r\\ p & 0 & r & -q\\ q & -r & 0 & p\\ r & q & -p & 0\end{bmatrix}\begin{bmatrix}q_0\\ q_1\\ q_2\\ q_3\end{bmatrix}+\varepsilon\begin{bmatrix}q_0\\ q_1\\ q_2\\ q_3\end{bmatrix} \qquad (1)$$

$$\varepsilon=1-\left(q_0^2+q_1^2+q_2^2+q_3^2\right)$$

where q_0, q_1 , q_2 e q_3 are the four elements of the quaternion [9] which describes the rotation aligning the vertical axes to the body ones; p, q and r are the three components of angular velocity vector of the body axes with respect to the vertical ones $\boldsymbol{\omega}^B$; ε is a corrective term used to avoid that the quaternion become different from 1 due to the numerical errors. The Euler angles are determined as follows:

$$\begin{cases}\varphi=\arctan\dfrac{2(q_0q_1+q_2q_3)}{q_0^2-q_1^2-q_2^2+q_3^2}\\ \vartheta=\arcsin[2(q_0q_2-q_1q_3)]\\ \psi=\arctan\dfrac{2(q_0q_3-q_1q_2)}{q_0^2+q_1^2-q_2^2-q_3^2}\end{cases} \qquad (2)$$

3.2 A/C Acceleration Calculation

The block evaluates an estimation of the A/C inertial acceleration ($\mathbf{a}^B$) which is used within the block "*Attitude & Heading Measurements*". As better explained in the next section, the last block provides an estimation of the Euler angles on the basis of the gravity vector components along the body axes ($\mathbf{g}^B$). However, to know such a vector it is necessary to purge the acceleration due to A/C manoeuvres from the measurements of the accelerometers.

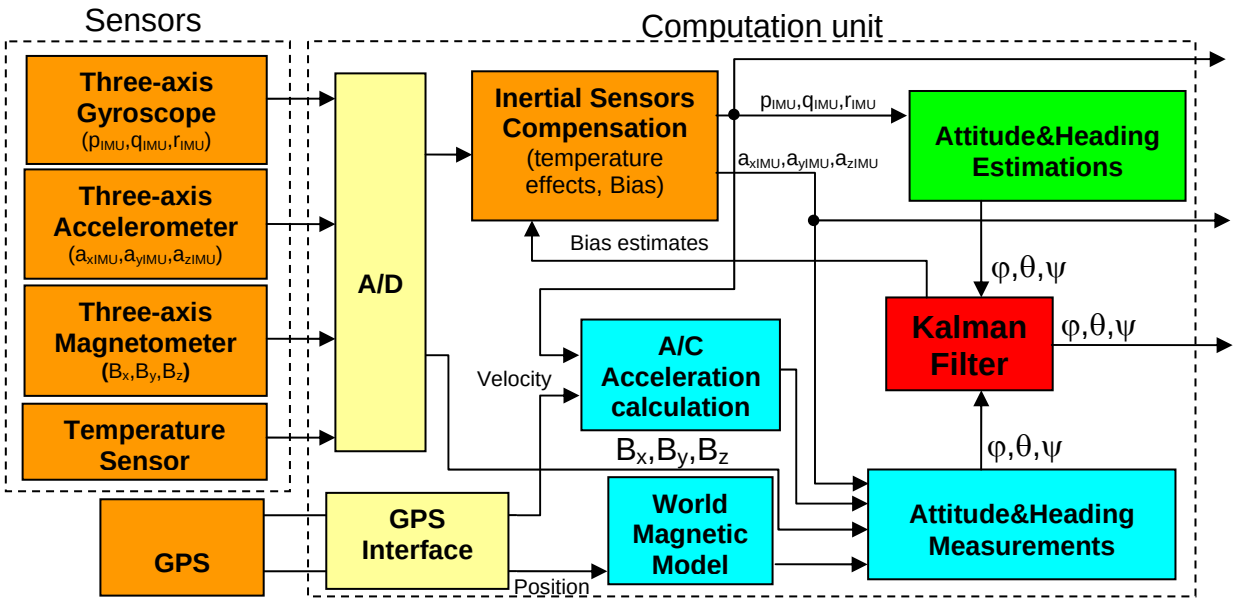

Fig. 1. The architecture of the developed AHRS

Under the approximation of non-rotating flat earth, the expression of the A/C acceleration vector is:

$$\mathbf{a}^B = \dot{\mathbf{v}}^B + \boldsymbol{\omega}^B \times \mathbf{v}^B \qquad (3)$$

where $\mathbf{v}^B$ is the velocity vector in body axes. The GPS data on velocity are provided in the vertical reference and therefore the related vector has to be rotated in body axes.
In principle, such an operation could be done by using the Euler angles estimated with equation (2), but such an approach establishes a correlation between these Euler angles and those "measured" through $\mathbf{g}^B$. Since the Kalman filter uses both information, the above mentioned correlation should cause the divergence of the filter itself. To overcome this problem the following simplification has been introduced:

$$\mathbf{v}^B = u\,\mathbf{i}, \quad (v = w = 0) \qquad (4)$$

where u is the modulus of the GPS velocity. In this way, (3) becomes:

$$\mathbf{a}^B = \dot{u}\,\mathbf{i} + ur\,\mathbf{j} - uq\,\mathbf{k} \qquad (5)$$

where $\dot{u}$ is calculated by doing the discrete derivate of two consecutive values of u.
Fig. 2 shows the results of the described model for a manoeuvre obtained with a flight simulator. It is worth noting that the behavior of the model is generally adequate, but there are some flight phases in which the errors increase substantially. In particular, since the discrete derivate is applied to the GPS low-frequency measurements, the approximation of the $\dot{u}$ (u_{dot} in Fig. 2) is inaccurate when rapid variations of the acceleration occur. For this reason, a specific *reject* algorithm (see section 3.5) has been developed to avoid the use of the model in such critical phases.

3.3 Attitude and Heading Measurements

The aim of this block is to supply an estimation of the Euler angles which does not depend on integration of the angular velocity measurements. Two different methods are used, named *Gauss-Newton* and *Master-Slave.*

Gauss-Newton method
This method is based on the knowledge of the components of the following vectors:

$$\mathbf{y}^V = \begin{bmatrix} 0 & 0 & g & B_N^V & B_E^V & B_D^V \end{bmatrix}$$
$$\mathbf{y}^B = \begin{bmatrix} g_x^B & g_y^B & g_z^B & B_x^B & B_y^B & B_z^B \end{bmatrix} \qquad (6)$$

where $\mathbf{g}^B = \left(g_x^B, g_y^B, g_z^B\right)$ is the gravity vector and $\mathbf{B}^B = \left(B_x^B, B_y^B, B_z^B\right)$ is the magnetic field

vector, both in the body reference frame, while $\mathbf{g}^V = (0,0,g)$ and $\mathbf{B}^V = (B_N^V, B_E^V, B_D^V)$ are the same vectors in the vertical reference frame. Vector $\mathbf{B}^V$ is given by the WMM, $\mathbf{B}^B$ is measured by the three-axis magnetometers installed on the strapdown platform and $\mathbf{g}^B$ comes from the following relationship:

$$\mathbf{g}^B = \mathbf{a}^B - \mathbf{a}_{\mathbf{IMU}} \tag{7}$$

where $\mathbf{a}_{\mathbf{IMU}}$ is the accelerometers measurement vector.

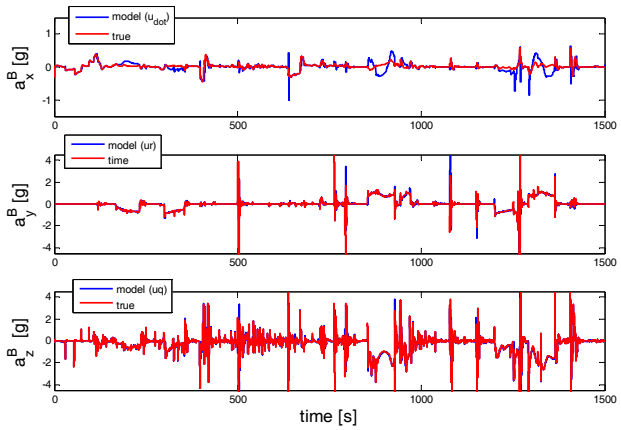

Fig. 2. Comparison between the true accelerations and estimated ones

By using the rotation matrix $\mathbf{T}_{V\to B}$ from vertical axes to body ones expressed in quaternion form:

$$\mathbf{T}_{V\to B} = \begin{bmatrix} q_0^2+q_1^2-q_2^2-q_3^2 & 2(q_1q_2+q_0q_3) & 2(q_1q_3-q_0q_2) \\ 2(q_1q_2-q_0q_3) & q_0^2-q_1^2+q_2^2-q_3^2 & 2(q_2q_3+q_0q_1) \\ 2(q_1q_3+q_0q_2) & 2(q_2q_3-q_0q_1) & q_0^2-q_1^2-q_2^2-q_3^2 \end{bmatrix} \tag{8}$$

it is possible to define the matrix $\mathbf{M}$ which allows the vector $\mathbf{y}^{\mathbf{V}}$ to be rotated in the body axes:

$$\mathbf{M} = \begin{bmatrix} \mathbf{T}_{V\to B} & 0_{3x3} \\ 0_{3x3} & \mathbf{T}_{V\to B} \end{bmatrix} \tag{9}$$

The mean square error is given by the function:

$$E = e^T e = \left(\mathbf{M}\mathbf{y}^V - \mathbf{y}^B\right)^T \left(\mathbf{M}\mathbf{y}^V - \mathbf{y}^B\right) \tag{10}$$

To find the quaternion which minimizes the error function (10), the *Gauss-Newton* method is used. It is worth noting that the model for the computation of the aircraft acceleration does not give a good estimation of the component of $\mathbf{g}$ along the axis Z^B because it neglects the term $\dot{w}$. For this reason the vector $\mathbf{y}$ has been reduced to 5 components rather than 6 by eliminating g_z^B. Consequently, the matrix $\mathbf{M}$ has been reduced to a [5x6] matrix by eliminating the third row.

The *Gauss-Newton* method evaluates the solution of interest through an iterative process which is stopped when the residuals of the quaternion components of two consecutive steps are lower than a fixed threshold value. The critical issue of this approach is the possibility that the method does not converge to the correct solution. For this reason it has been necessary to develop the alternative method.

Master-Slave method

The basic idea is to evaluate θ and φ from $\mathbf{g}^B$ and ψ from $\mathbf{B}^B$.

Pitch and roll angles are evaluated through the following relations (*Master* computation):

$$\begin{aligned} \vartheta &= -\arcsin\frac{g_x^B}{g} \\ \varphi &= k\pi - \arcsin\frac{g_y^B}{g\cos\vartheta} \end{aligned} \tag{11}$$

where

$$\begin{aligned} &k = 0 \quad \text{for} \quad g_z^B > 0 \\ &k = 1 \quad \text{for} \quad g_z^B < 0 \text{ and } g_y^B > 0 \\ &k = -1 \quad \text{for} \quad g_z^B < 0 \text{ and } g_y^B < 0 \\ &k \text{ undefined for } g_z^B = 0 \end{aligned}$$

It is worth noting that the roll angle could be also evaluated by using g_z^B in place of g_y^B, however the latter is preferable because, as already stated, the quality of the estimation of g_z^B is quite poor.

Once the pitch and roll angles are known, it is possible to calculate the components of vector $\boldsymbol{B}^B$ in an intermediate reference frame F' as follows:

$$\mathbf{B}^{F'} = \mathbf{T}_{B\to F'}\,\mathbf{B}^B \tag{12}$$

where

$$\mathbf{T}_{B\to F'} = \begin{bmatrix} \cos\vartheta & 0 & \sin\vartheta \\ 0 & 1 & 0 \\ -\sin\vartheta & 0 & \cos\vartheta \end{bmatrix} \begin{bmatrix} 1 & 0 & 0 \\ 0 & \cos\varphi & -\sin\varphi \\ 0 & \sin\varphi & \cos\varphi \end{bmatrix} \tag{13}$$

and, finally, under the approximation that the terrestrial magnetic field is aligned with X^V, it is possible to determine ψ from the following relationships:

$$\begin{aligned} B_x^{F'} &= B_N^V \cos\hat{\psi} \\ B_y^{F'} &= -B_N^V \sin\hat{\psi} \end{aligned} \qquad (14)$$

The method provides the heading angle with respect to the magnetic meridian ($\hat{\psi}$) which has to be corrected for the magnetic declination given by the WMM.

Fig. 3 shows a comparison between the two models, with reference to the same manoeuvre considered in Fig. 2. The behaviour of *Gauss-Newton* method is generally better, but both techniques have considerable errors during the flight phases characterized by high accelerations.

The *Master-Slave* is used during the phase named "alignment", that is at the turning on of the system, to establish the integration initial conditions of the rotation quaternion. In addition, it is used at the activation of the *reset* function which will be described in section 3.5. In all the other operative conditions the system calculates the "measured" values through the *Gauss-Newton* method.

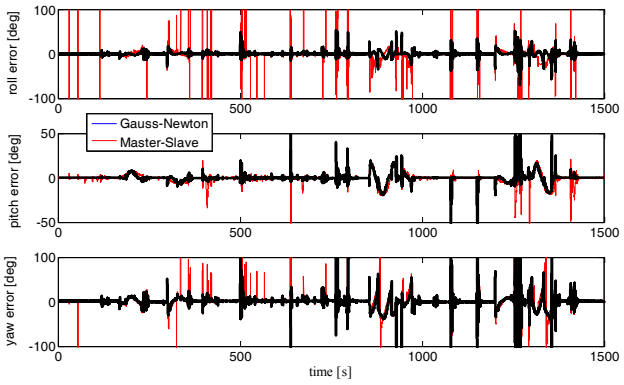

Fig. 3. Comparison between the *Gauss-Newton* and *Master-Slave* methods

3.4 The Kalman Filter

The block Kalman filter is an iterative algorithm [5] which allows the optimum estimation of attitude and heading through the analysis of data provided by two different sources: the integration of differential equations (1) and the models described in the previous paragraph. The goal of the filter is to calculate the four error components of the rotation quaternion and the three bias errors of the gyroscopes:

$$\delta\mathbf{x} = \left[\delta q_0 \quad \delta q_1 \quad \delta q_2 \quad \delta q_3 \quad \delta b_x \quad \delta b_y \quad \delta b_z\right]^{\mathrm{T}} \qquad (15)$$

The knowledge of the bias errors is relevant for those flight phases in which the attitude and heading measurements are characterized by small precision. As it will be described in the next section, the system has adequate algorithms to identify such conditions, during which the Euler angles are calculated with the only integration of the angular velocities. Consequently, the possibility to correct the gyroscopes measurements from the bias errors allows the errors on the Euler angles to be limited. The recursive computation of data affected by errors bases on the knowledge of a mathematic model of the examined phenomenon and its errors, and on the characterization of the measurement errors. The characteristic equation of quaternion errors is obtained by linearizing equation (1) which can be written in a vector form:

$$\begin{cases} \dot{\mathbf{x}}_\mathbf{q} = \mathbf{f}_\mathbf{q}\left(\mathbf{x}_\mathbf{q}, \mathbf{u}\right) \\ \mathbf{q} = \mathbf{H}_\mathbf{q}\mathbf{x}_\mathbf{q} \end{cases} \qquad (16)$$
$$\mathbf{x}_\mathbf{q} = \left[q_0 \quad q_1 \quad q_2 \quad q_3\right]^{\mathrm{T}};$$
$$\mathbf{u} = \left[0 \quad p \quad q \quad r\right]^{\mathrm{T}}; \quad \mathbf{H}_\mathbf{q} = \mathbf{I}_{4\mathrm{x}4}$$

By introducing the perturbation quantities for the state vector ($\boldsymbol{\delta}\mathbf{x}_\mathbf{q}$) and input vectors ($\boldsymbol{\delta}\mathbf{u}$):

$$\begin{aligned} \mathbf{x}_\mathbf{q} &= \bar{\mathbf{x}}_\mathbf{q} + \boldsymbol{\delta}\mathbf{x}_\mathbf{q} \\ \mathbf{u} &= \bar{\mathbf{u}} + \boldsymbol{\delta}\mathbf{u} \end{aligned} \qquad (17)$$

and by stopping to the first order the power series of Taylor of the $\mathbf{f}_\mathbf{q}$, the quaternion error equation is determined:

$$\begin{cases} \boldsymbol{\delta}\dot{\mathbf{x}}_\mathbf{q} = \mathbf{F}_\mathbf{q}\boldsymbol{\delta}\mathbf{x}_\mathbf{q} + \mathbf{G}_\mathbf{q}\boldsymbol{\delta}\mathbf{u} \\ \boldsymbol{\delta}\mathbf{q} = \mathbf{H}_\mathbf{q}\boldsymbol{\delta}\mathbf{x}_\mathbf{q} \end{cases} \qquad (18)$$

where the matrix $\mathbf{F}_\mathbf{q}$ (the terms referred to ε are neglected on the diagonal) and $\mathbf{G}_\mathbf{q}$ are constituted by the following terms:

$$\mathbf{F_q} = \left.\frac{\partial \mathbf{f_q}}{\partial \mathbf{x_q}}\right|_{\bar{\mathbf{x}}_\mathbf{q},\bar{\mathbf{u}}} =$$

$$= \begin{bmatrix} -2q_0^2 & -\frac{p}{2}-2q_0q_1 & -\frac{q}{2}-2q_0q_2 & -\frac{r}{2}-2q_0q_3 \\ \frac{p}{2}-2q_0q_1 & -2q_1^2 & \frac{r}{2}-2q_1q_2 & -\frac{q}{2}-2q_1q_3 \\ \frac{q}{2}-2q_0q_2 & -\frac{r}{2}-2q_1q_2 & -2q_2^2 & \frac{p}{2}-2q_2q_3 \\ \frac{r}{2}-2q_0q_3 & \frac{q}{2}-2q_1q_3 & -\frac{p}{2}-2q_2q_3 & -2q_3^2 \end{bmatrix}_{\bar{\mathbf{x}}_\mathbf{q},\bar{\mathbf{u}}} \quad (19)$$

$$\mathbf{G_q} = \left.\frac{\partial \mathbf{f_q}}{\partial \mathbf{u}}\right|_{\bar{\mathbf{x}}_\mathbf{q},\bar{\mathbf{u}}} = \begin{bmatrix} -\frac{q_1}{2} & -\frac{q_2}{2} & -\frac{q_3}{2} \\ \frac{q_0}{2} & -\frac{q_3}{2} & \frac{q_2}{2} \\ \frac{q_3}{2} & \frac{q_0}{2} & -\frac{q_1}{2} \\ -\frac{q_2}{2} & \frac{q_1}{2} & \frac{q_0}{2} \end{bmatrix}_{\bar{\mathbf{x}}_\mathbf{q},\bar{\mathbf{u}}}$$

In this work the measurement errors of the gyroscopes are constituted by a bias term and a part of white noise, and they are modeled through the linear process of Wiener [5]. Thus, the analogous model of equation (18) for the gyroscopes errors is:

$$\begin{cases} \dot{\delta\mathbf{x}}_\mathbf{b} = \mathbf{F_b}\delta\mathbf{x_b} + \mathbf{G_b}\boldsymbol{\eta} \\ \delta\mathbf{b} = \mathbf{H_b}\delta\mathbf{x_b} + \boldsymbol{\upsilon} \end{cases} \quad (20)$$
$$\delta\mathbf{b} = \begin{bmatrix} \delta b_x & \delta b_y & \delta b_z \end{bmatrix}^\mathrm{T}; \quad \mathbf{F_b} = 0_{3x3}; \quad \mathbf{G_b} = \mathbf{H_b} = \mathbf{I}_{3x3}$$

where $\boldsymbol{\eta}$ is the white noises vector of the Wiener process and $\boldsymbol{\upsilon}$ is the white noises vector of the gyroscopes measurements. The perturbation model used by the filter is the union of the models expressed by (18) and (20):

$$\dot{\delta\mathbf{x}} = F\delta\mathbf{x} + \mathbf{G}\mathbf{w} = \begin{bmatrix} \mathbf{F_q} & \mathbf{G_q}\mathbf{H_q} \\ \mathbf{0}_{3x3} & \mathbf{F_b} \end{bmatrix} \begin{bmatrix} \delta\mathbf{x_q} \\ \delta\mathbf{x_b} \end{bmatrix} + \begin{bmatrix} \mathbf{G_q} & \mathbf{0}_{4x3} \\ \mathbf{0}_{3x3} & \mathbf{G_b} \end{bmatrix} \begin{bmatrix} \boldsymbol{\upsilon} \\ \boldsymbol{\eta} \end{bmatrix} \quad (21)$$

Starting from that which generally is named "prediction" estimation of the unknown state ($\delta\hat{\mathbf{x}}_\mathbf{k}^-$), the system calculates the optimum value at the instant t_k ($\delta\hat{\mathbf{x}}_\mathbf{k}$) by means of the classic relation of the Kalman filter theory [5]:

$$\delta\hat{\mathbf{x}}_\mathbf{k} = \delta\hat{\mathbf{x}}_\mathbf{k}^- + \mathbf{K_k}\left(\delta\mathbf{z_k} - \mathbf{H}\delta\hat{\mathbf{x}}_\mathbf{k}^-\right); \quad \mathbf{H} = \begin{bmatrix} \mathbf{I}_{4x4} & 0_{3x3} \end{bmatrix} \quad (22)$$

where $\delta\mathbf{z_k}$ is the difference in terms of quaternion between the attitude and heading "measured" vector and the attitude and heading "estimated" vector. The Kalman gain matrix $\mathbf{K_k}$ is determined with the following expression on the basis of the correlation matrix of the errors ($\mathbf{P}_\mathbf{k}^-$):

$$\mathbf{K_k} = \mathbf{P}_\mathbf{k}^-\mathbf{H}^\mathrm{T}\left(\mathbf{H}\mathbf{P}_\mathbf{k}^-\mathbf{H}^\mathrm{T} + \mathbf{R_k}\right)^{-1} \quad (23)$$

where $\mathbf{R_k}$ is the correlation matrix of the noise measurements. By using the optimum estimation $\delta\hat{\mathbf{x}}_\mathbf{k}$, the prediction value to be adopted to next step in (22) is given by:

$$\delta\hat{\mathbf{x}}_{\mathbf{k+1}}^- = \boldsymbol{\Phi}_\mathbf{k}\delta\hat{\mathbf{x}}_\mathbf{k} \quad (24)$$

By considering a small range (t_k- t_{k-1}), the transition matrix $\boldsymbol{\Phi}_\mathbf{k}$ can be approximated in power series (generally stopped to the first order):

$$\boldsymbol{\Phi}_\mathbf{k} = \mathbf{e}^{\mathbf{F}t} = \mathbf{I} + \mathbf{F}\left(t_k - t_{k-1}\right) + \frac{\mathbf{F}^2\left(t_k - t_{k-1}\right)^2}{2!} + o^3; \quad (25)$$

The transition matrix is also used to calculate the prediction value of the correlation matrix of the errors:

$$\mathbf{P}_{\mathbf{k+1}}^- = \mathbf{E}\left[\mathbf{x}_{\mathbf{k+1}}^-\left(\mathbf{x}_{\mathbf{k+1}}^-\right)^\mathrm{T}\right] = \Phi_\mathbf{k}\mathbf{P_k}\Phi_\mathbf{k}^\mathrm{T} + \mathbf{Q_k} \quad (26)$$

Such a matrix is used in (23) for the next step.

3.5 Reject and Reset Functions

As previously stated, there are some flight phases in which the Euler angles provided by the "*Attitude & Heading Measurements*" model show large errors. The *reject* function has the goal to identify such flight phases in order to avoid that the Kalman filter processes the data given by such a block. In the case of rejection, the execution of the filter is delayed until the data return valid. As a consequence, the evaluation of the Euler angles is fully devolved to the integration of the angular velocities. The bias errors calculated by the Kalman filter before the activation of the *reject* are stored and used during these phases. A validity test compares the Euler angles "measured" with those "estimated". If one of the three differences is higher than a fixed threshold, the "measured" values are discarded. The threshold value has been fixed to 20 deg on the basis of simulation tests results. Such a value is a compromise between to guarantee an adequate rejection of non-valid measurements and to limit the risk of divergence of the Kalman filter.

The other function, called *reset*, sets the outputs of the AHRS equal to those provided by the

"*Attitude & Heading Measurements*" model in case the latter show high accuracy. The goal of this function is to provide to the system reliable data in order to reset the errors of the filter. The function is applied during the flight phases approximately characterized by a quasi-rectilinear uniform motion. The system declares such conditions if both the following relations are verified:

$$\left|\left\|\mathbf{A}_{\mathbf{IMU}}\right| - g\right| \le a_{th} \text{ and } \left|\boldsymbol{\omega}_{\mathbf{IMU}}\right| \le \omega_{th} \qquad (27)$$

where the threshold values a_{th} and ω_{th}, chosen thanks to simulation tests, are 0.005 m/s^2 and 0.05°/s, respectively. The reset values are calculated with the *Master-Slave* method as a consequence of its high reliability in the presence of small accelerations.

4 Results

In this chapter some results of AHRS simulation tests are illustrated. By performing some manoeuvres with a flight simulator, time histories of acceleration, velocity and position of an aircraft have been generated. Such data have been "dirtied" using the error models described in section 2. A Matlab-Simulink model implementing the AHRS has been developed to process the input data. A subset of such inputs histories have been used for the calibration of the system parameters, while the other ones have been used for the performance assessment. Maximum, mean and minimum errors, together with the root mean square (RMS) error, have been chosen as performance parameters. Fig. 4 shows an example of the simulation results related to the reference manoeuvre already considered in the previous sections.

It is worth noting that the errors are always small (less than 2 deg on each Euler angle) and thus a suitable performance is also guaranteed during the flight phases characterized by strong accelerations.

Such good results have been obtained using the AHRS with all the functions active. Several simulation tests have been carried out in order to assess the importance of the various functions developed. In particular, the effects of eliminating from the system the *reject* function or the GPS has been evaluated.

If the GPS is not available it is not possible to estimate $\mathbf{a}^B$ in (7).

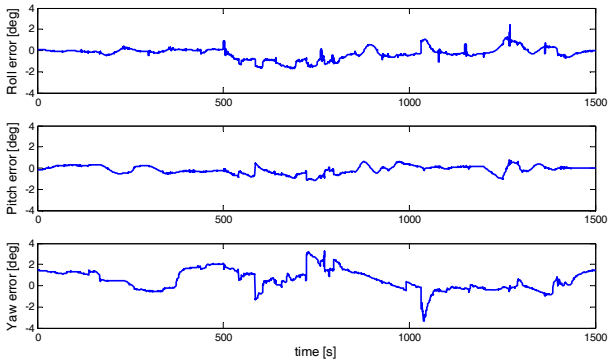

Fig. 4. Example of simulation test results

Tab. 3 illustrates the RMS, the maximum and the mean of the errors on the three Euler angles referred to a set of manoeuvres, obtained with different AHRS configurations. It is possible to notice that if the *reject* function and the GPS are not active the errors dramatically increase. By using them separately, a reduction of the mean and RMS errors is obtained, but not of the maximum errors. However, to obtain a considerable reduction of maximum errors it is necessary to couple the *reject* function with the use of the GPS.

GPS	Reject	RMS Error (°)			Mean Error (°)			Maximum Error (°)		
		Roll	Pitch	Yaw	Roll	Pitch	Yaw	Roll	Pitch	Yaw
off	off	2.47	1.89	5.15	0.147	0.256	3.26	18.4	18.1	19.5
on	off	0.924	0.981	2.29	0.272	0.043	0.266	5.15	7.71	18.3
off	on	0.651	0.561	1.37	0.141	0.139	0.272	3.40	3.67	8.38
on	on	0.438	0.450	0.836	0.138	0.059	0.207	3.13	2.87	4.76

Tab. 3. AHRS performance evaluated on a set of simulation manoeuvres

This is because the *reject* function allows inaccurate attitude and heading "measurements" to be not used by the system. On the other hand, a good prediction of the bias errors permits to limit the errors when the Kalman filter is not active.

Some simulation tests have been carried out also in order to evaluate the importance of the *reset* function. The results show that such an effect is

negligible since the error level of restarting values is comparable with that of system outputs which is already acceptable.

5 Conclusions

This work aimed to develop an *Attitude & Heading Reference System* able to achieve high accuracy during all the flight phases of high performance aircrafts or UAV. The system is based on a Kalman filter which processes data coming from a multi-sensor architecture, constituted by gyroscopes, accelerometers, magnetometers, a temperature sensor and a GPS receiver. Such an architecture provides two different estimations of the Euler angles that are used by the filter to correct the errors.

The architecture and the methodologies developed to limit the errors demonstrated their validity. The system has shown satisfactory performance and small errors during simulated aircraft maneuvers. This is mainly due to the use of the GPS together with a *reject* function. The GPS allows the aircraft acceleration to be estimated. This permits the calculation of the gravity vector from the accelerometers during aircraft maneuvers, increasing the accuracy of Euler angles computation based on accelerometers and magnetometers. The *reject* function temporarily switches off the Kalman filter when a too large difference occurs between the two estimations of the Euler angles used by the filter itself. In this way, it avoids possible divergences of the filter without using complex architectures (e.g. filter gains variable with flight conditions).

A *reset* function, able to restart the filter, during quasi-uniform rectilinear flight phases, has been tested too. Nevertheless, the effect of this function is negligible since the error level of restarting values is comparable with that of system outputs which is already acceptable.

References

[1] P. S. Maybeck, *Stochastic Models, Estimation, and Control*. Academic Press, Volume 1, 1979.

[2] J. Farrell, M. Barth. *The Global Positioning System and Inertial Navigation*. McGraw-Hill, 1999.

[3] M. S. Grewal, L. R. Weill, A. P. Andrews. *Global Positioning Systems, Inertial Navigation, and Integration*. John Wiley & Sons, 2001.

[4] A. Lawrence. *Modern Inertial Technology: Navigation, Guidance, and Control*. Springer, Second Edition, 1998.

[5] R. G. Brown, P. Y. C. Hwang. *Introduction to Random Signals and Applied Kalman Filtering*. John Wiley & Sons, Second Edition, 1992.

[6] B. W. Parkinson, J. J. Spilker. *Global Positioning System: Theory and Applications Volume 1*. American Institute of Aeronautics and Astronautics, Progress in Astronautics and Aeronautics Volume 163, 1996.

[7] B. W. Parkinson, J. J. Spilker. *Global Positioning System: Theory and Applications Volume 2*. American Institute of Aeronautics and Astronautics, Progress in Astronautics and Aeronautics Volume 164, 1996.

[8] S. McLean, S. Macmillan, S. Maus, V. Lesur, A. Thomson, D. Dater. *The US/UK World Magnetic Model for 2005-2010*, NOAA Technical Report NESDIS/NGDC-1, 2004.

[9] B. L. Stevens, F. L. Lewis. *Aircraft Control and Simulation*. John Wiley & Sons, Second Edition, 2003.

Copyright Statement